Astrometry and photometry in high contrast imaging: ADI/LOCI biases and the SOSIE/LOCI solution

Raphaël Galicher[1,2,a] and Christian Marois[1]

[1] National Research Council Canada, Herzberg Institute of Astrophysics, 5071 West Saanich Road, Victoria, BC, V9E 2E7, Canada
[2] Dept. de Physique, Université de Montréal, C.P. 6128 Succ. Centre-ville, Montréal, Qc, H3C 3J7, Canada

Abstract. The direct exoplanet imaging field will strongly benefit from the higher angular resolution achieved by next generation 30+m telescopes. To fully take advantage of these new facilities, one of the biggest challenges that ground-based adaptive optics imaging must overcome is to derive accurate astrometry and photometry of point sources. The planet photometry and its astrometry are used to compare with atmospheric models and to fit orbits. If erroneous numbers are found, or if errors are underestimated, spurious fits can lead to unphysical planet characteristics or wrong/unstable orbits. Overestimating the errors also needs to be avoided as it degrades the value of the data. Several photometry/astrometry biases that are induced by advance imaging and processing techniques (such as ADI/SSDI/LOCI) are presented as well as a procedure to properly overcome those effects. These solutions will be implemented in the Gemini Planet Imager campaign data pipeline and it is expected that they will also play a crucial role in any future direct exoplanet imaging survey.

1 Introduction

Several techniques have been used to detect exoplanets. All these methods have their limitations and probe different regimes of planet mass and separation. For example, radial velocity and transit surveys are more efficient on exploring close-in planets ($\lesssim$5 AU). Direct imaging focuses on long-period/wide orbit young and massive planets ($\gtrsim$5 AU) [1–4]. The two widely used observation modes for direct imaging are the angular differential imaging (ADI, [5]) and the simultaneous spectral differential imaging (SSDI, [6, 7]) techniques. The data obtained by these observing modes require a specific processing to achieve high contrast. One of the most efficient PSF subtraction algorithm used for these type of data is the locally optimized combination imaging technique (LOCI, [8]). The LOCI technique has become common, and easy-to-use "black box" are often used to obtain high contrast imaging of exoplanets. However, ADI or SSDI data processing techniques may introduce peculiar biases that impact the values obtained when trying to derive accurate astrometry and photometry of candidates. In this paper, the SOSIE pipeline ([9], § 2) is presented, various ADI and LOCI undesirable effects are then investigated (§ 3) and a method to overcome the biases on the photometry and astrometry of exoplanets is finally described (§ 4).

2 The SOSIE pipeline

High contrast imaging is usually limited by quasi-static speckles that are created by slow drifts in time of the phase and amplitude aberrations on the optics in the telescope and instruments. In future instruments dedicated to direct imaging of exoplanets, like GPI [10] or SPHERE [11], an additional calibration stage will properly estimate these aberrations at the science wavelength and correct them using a high-order deformable mirror. In current instrument, this stage does not exist and the calibration relies entirely on post-processing of the data. The ADI observation mode has been developed to calibrate the quasi-static speckles. It consists of setting the telescope instrument rotator to track the telescope pupil on an altitude/azimuth mount telescope. A sequence of exposures is then acquired on the target (left in Fig. 1). As the camera and the telescope optics are aligned for all exposures, the

[a] raphael.galicher 'at' nrc-cnrc.gc.ca

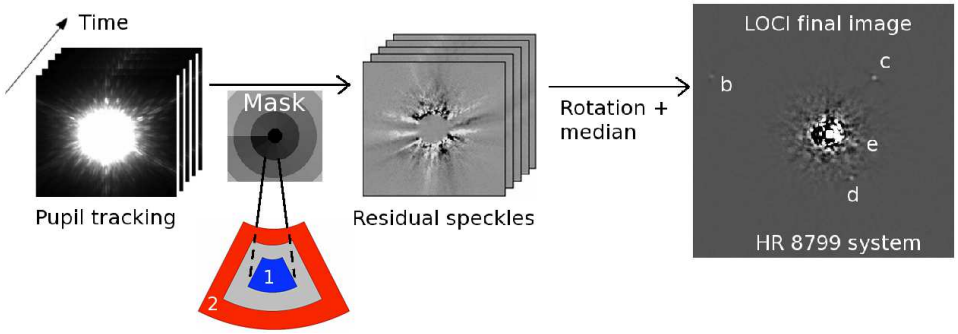

Fig. 1. ADI LOCI/SOSIE principle.

speckle pattern is stable in time and can be accurately estimated and subtracted using the other images of the sequence. Since the telescope has an altitude/azimuth mount and the instrument rotator is setup to track the telescope pupil, any off-axis source will slowly revolve with time around the target star. A LOCI algorithm is then used to process the images of the sequence one by one to keep what is revolving with time (planets) and remove anything that is static with time (speckles). Each image is divided in sections of interest where the speckle noise is calibrated (see mask in Fig. 1). For each section of an image, the LOCI algorithm search for the linear combination of other images of the sequence (where images acquired too close in time to the image of interest are avoided to minimize candidates self-subtraction) to produce an optimal reference speckle pattern to subtract to the region 1. In the first version of the algorithm, the minimization was done in the section of interest [8] (region 1). It has been showed that the presence of an off-axis source in the section of interest may bias the subtraction and partially remove flux from the candidate. The SOSIE pipeline was developed [9] to avoid this effect. The upgraded algorithm finds the linear combination that minimizes the noise in a region (region 2 in Fig. 1) around the section of interest (region 1). As the speckles are spatially correlated, noise is also minimized in the region of interest. Once the speckle subtraction has been done in all sections of all images of the sequence (residual speckles in Fig. 1), all images are rotated to align their North angle and they are median-combined. Planets not visible in any single unsubtracted image can now be detected as in the case of the HR 8799 four planets (right image).

3 Astrometry and photometry biases

3.1 Impact of smearing in ADI sequences

When taking images in the ADI mode, the instrument rotator is set to track the telescope pupil, generating a non-linear field-of-view (FOV) rotation with time. For fast FOV rotation cases (near Zenith transits), the image of an off-axis source will be moving on the detector during a single exposure, generating an azimuthally smeared point-spread function. Far from the transit, the FOV rotates very slowly and the off-axis source image is very similar to the point-spread function (PSF) of the instrument (left, Fig. 2). Closer to the transit, the azimuthal spread is larger because the FOV rotates faster (center). At the transit, the off-axis source PSF can be spread over a large number of pixels (right). The flux of the off-axis source is not constant during the sequence. To show the impact of smearing, we consider the central unsaturated PSF of HR 8799 in a typical NIRC2 sequence. We create a fake sequence shifting the PSF at the position of HR 8799c accounting for the field-of-view rotation and the smearing in each image (only the off-axis source is present in the data cube). We then plot the maximum of the fake planet during the sequence in Fig. 3. At transit, the maximum of the image is 30% less than the unsaturated PSF because of smearing. Further from transit, oscillations appear when the off-axis source image goes from one pixel to its neighbor on the detector. The maximum of the final image (median combination of the cube) is 6% less than the maximum of the unsaturated PSF. The loss in flux is the same if we consider the integrated flux in a 1 PSF diameter area. The values are even worst for sources

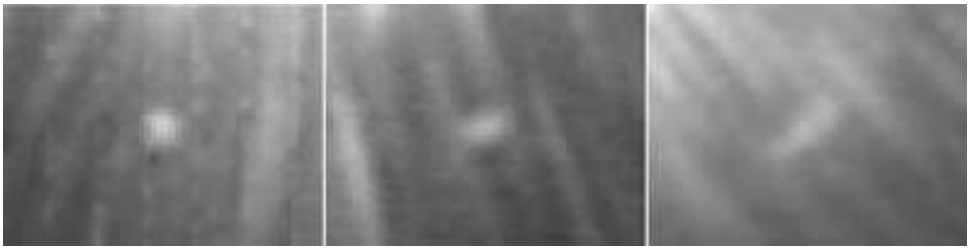

Fig. 2. ADI off-axis source image (HR 8799b) in raw data far from (left), closer to (center) and at (right) the transit. Data were taken at KECKII with NIRC2.

that are further from the central star and it is important to estimate the amount of signal that is lost by the smearing.

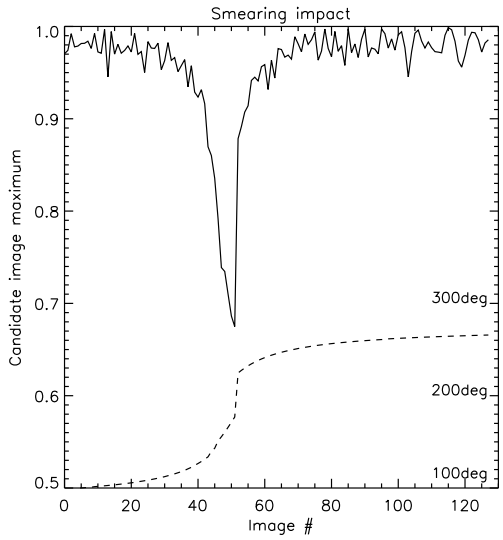

Fig. 3. Maximum of an off-axis source during the sequence. Values are normalized to the unsaturated on-axis PSF. The dashed line gives the angle to north of each image in degrees (scale on the right).

3.2 LOCI distortions and throughput

The LOCI procedure does produce additional biases. For any section in any image of the sequence, a linear combination of the other images is used to subtract the speckles (§ 2). Let call $\alpha_{i,j,S}$ the LOCI coefficient applied to image j (I_j) in the linear combination when subtracting the speckle noise in section S of image i (I_i). The resulting flux R_i in image i after subtraction is

$$R_i = \sum_S \left(I_i - \sum_j \alpha_{i,j,S} \; I_j \right) S \tag{1}$$

In any image of the residual speckle cube (Fig. 1), the off-axis source image looks like the image in the left panel of Fig. 4. The white spot is the source image in I_i and the dark wings come from the subtraction of other images I_j of the sequence where the source has moved around the target star. As the $\alpha_{i,j,S}$ coefficients change from a frame to an other, the image of a given off-axis source evolves in the sequence. The last step of the LOCI procedure median-combines all the images of the sequence

and give a very typical pattern for an off-axis source (center in Fig. 4). If the LOCI parameters that set the section shapes are modified, the coefficients change and the resulting image of the off-axis source also changes (right).

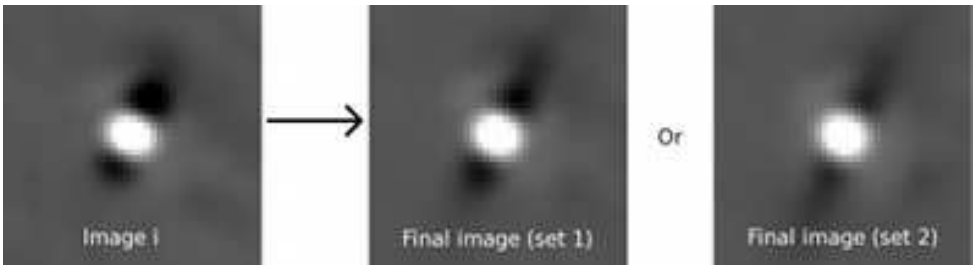

Fig. 4. LOCI off-axis source image (HR 8799b) in one image of the residual speckle cube (left) and in the final LOCI image for two different sets of LOCI parameters (center and right). Data were taken at KECKII with NIRC2.

4 Determining accurate photometry and astrometry on LOCI images

As shown in the previous section, the smearing impacts the flux estimation in any ADI sequence. Moreover, the pattern of an off-axis source in the final LOCI image can significantly change for various LOCI parameters. An optimal procedure to account for the various biases is needed for each detected off-axis source if accurate astrometry and photometry is to be retrieved. With SOSIE, an unsaturated PSF of the central star is recorded along with the ADI sequence. When processing the data, the LOCI procedure is first applied to reduce the speckle noise while saving the LOCI coefficients for all sections of all images. If an off-axis source is detected in the final median-combined image, a rough estimate for its position and flux is estimated by hand or by fitting a Gaussian function. The unsaturated PSF is then used to build a sequence of simulated candidate images at the rough position accounting for the FOV smearing in each exposure. The recorded LOCI coefficients are then used to generate a LOCI PSF, the images are then rotate and median-combined. The result is a template that estimates the off-axis PSF image in the final LOCI image (Fig. 5). The LOCI PSF template is used

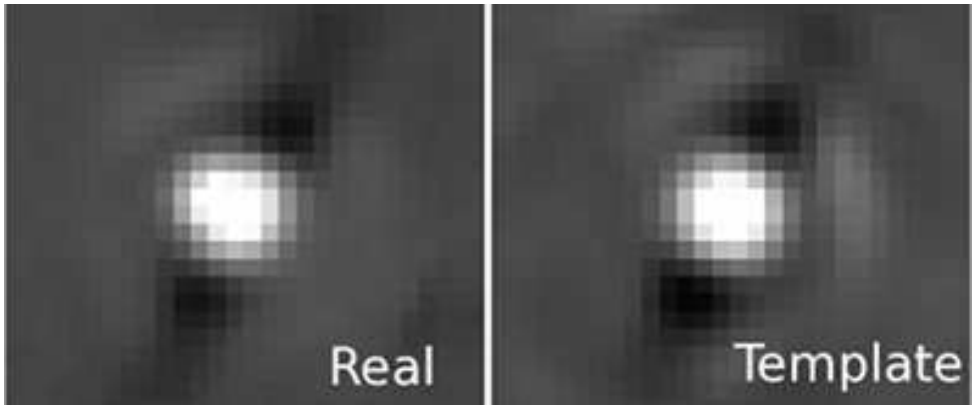

Fig. 5. Real LOCI off-axis source image (HR 8799b, left) and its template (right). Data from KECKII with NIRC2.

to derive the candidate flux (m_0) and its position relative to the star (x_0, y_0) by iteratively subtracting it from the real image to search for the set of parameters that minimizes the local noise. For each

parameter set, the local residual subtraction noise κ is calculated in a disk of 2 PSF diameter (Fig. 6). Once the triplet that minimizes the residuals has been found, the error on each parameter is estimated

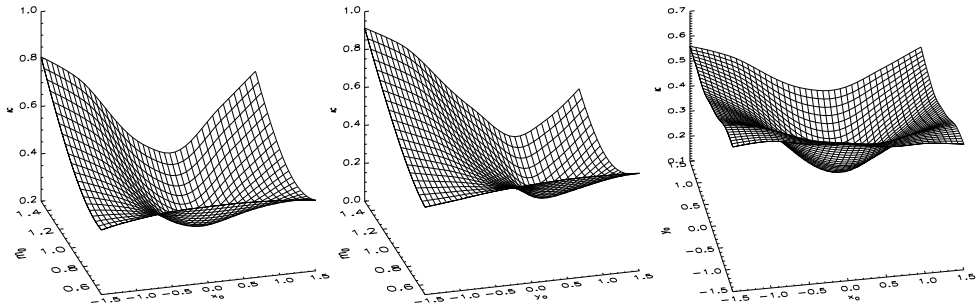

Fig. 6. Residual level as function of (x_0, m_0) (left), (y_0, m_0) (center) and (x_0, y_0) (right).

by searching for nearby set of parameters that increase the minimum residual level by a factor of $\sqrt{2}$. These ranges are defined as the 1σ errors of the measurements. It is interesting to notice that these errors include the error due to a difference between the unsaturated PSF used to create the simulated candidate and the real PSFs (distortion variation when the candidate moves on the detector during the sequence). If the PSFs are very different, κ slowly evolves and the minimum is not well defined. To illustrate the interest of the LOCI template fitting, we follow the procedure describe in §3 to create a fake planet and we add it to the KECK HR 8799 sequence. We put the planet at the symmetric position of HR 8799c with respect to the East-West axis. Its contrast is set to 10^{-4}. We apply the SOSIE pipeline to obtain the LOCI image and detect the planet. We roughly estimate its position and run the fitting procedure (creates and fits the LOCI template to the image) to retrieve the candidate photometry and astrometry. As a comparison, we perform the fit of the central unsaturated PSF to the LOCI image. We use the same procedure to estimate the error bars in both cases (Fig. 6). Results are given in Tab. 1. The planet astrometry and photometry are well retrieved with the SOSIE/LOCI procedure with accuracy and small error bars. The error bars are usually a bit larger (0.1-0.5 pixel) on a real candidate because of uncorrected distortions (not simulated with the fake candidate we added). Without the SOSIE procedure, the estimated position is within the 1σ error bars. However, as the unsaturated PSF is far from having the LOCI off-axis source shape, the minimization of noise within a 2 PSF area gives error bars that are ∼10 times larger than with the SOSIE/LOCI procedure. For the same reason, the contrast error bar is ∼ 30 times larger than when the SOSIE procedure is applied. But even with such a large error bar the estimated contrast is underestimated by more than 2σ. It is thus very important to account

	Real	SOSIE/LOCI	Error	Direct PSF fit	Error
x(pix)	58.00	58.00±0.10	0.003	58.11±1.03	0.11
y(pix)	-74.00	-74.02±0.10	0.016	-74.28±1.18	-0.28
Contrast $\times 10^4$	1	0.990±0.009	1%	0.46±0.25	54%

Table 1. *Astrometry and photometry estimated by the SOSIE/LOCI pipeline and by the unsaturated PSF fit for a fake planet around HR 8799 in a real KECK sequence. x and y are the x- and y-position from the central star. The Error columns give the excursion from the real values.*

for the smearing within exposures and for the LOCI distortions when retrieving the astrometry and photometry.

5 Conclusion

This preliminary study was performed to highlight various pitfalls of using ADI and LOCI when trying to estimate accurate astrometry and photometry of off-axis point sources. It was showed that with ADI, non-linear PSF smearing can impact the measured parameters. The LOCI procedure also biases the photometry and astrometry if the candidate flux is part of the LOCI correlation matrix calculation and by producing specific negative wings (from candidate partial self-subtraction) around candidates. We showed that fitting a simple PSF or Gaussian function to an off-axis source in ADI/LOCI image in order to retrieve its photometry and astrometry is strongly biased. We thus proposed a solution that calibrates the ADI and LOCI biases by using template smeared LOCI PSFs and that provides an estimation of the astrometry and photometry with error bars. As the problematic is the similar, the SOSIE solution can be applied to SSDI data. A more complete study of the biases induced in ADI/SSDI/LOCI images as uncorrected distortions, anisoplanetism, seeing evolution, telescope position with respect to the local zenith, or central star position on the detector will be presented in a forthcoming paper.

References

1. Marois, C. et al., Science, **322**, (2008) 1348-.
2. Kalas, P. et al., Science, **322**, (2008) 1345-.
3. Lagrange, A.-M. et al., Astronomy & Astrophysics, **493**, (2009) L21-L25.
4. Marois, C., and Zuckerman, B., and Konopacky, Q. M., and Macintosh, B., and Barman, T., Nature, **468**, (2010) 1080-1083.
5. Marois, C., and Lafrenière, D., and Doyon, R., and Macintosh, B., and Nadeau, D., The Astrophysical Journal, **641**, (2006) 556-564.
6. Racine, R., and Walker, G. A. H., and Nadeau, D., and Doyon, R. and Marois, C., Publications of the Astronomical Society of the Pacific, **111**, (1999) 587-594.
7. Marois, C., and Doyon, R., and Racine, R., and Nadeau, D., Publications of the Astronomical Society of the Pacific, **112**, (2000) 91-96.
8. Lafrenière, D., and Marois, C., and Doyon, R., and Nadeau, D., and Artigau, E., The Astrophysical Journal, **660**, (2007) 770-780.
9. Marois, C., and Macintosh, B., and Véran, J.-P., Society of Photo-Optical Instrumentation Engineers (SPIE) Conference Series, **7736**, (2010).
10. Macintosh, B. et al., Society of Photo-Optical Instrumentation Engineers (SPIE) Conference Series, **7015**, (2008).
11. Beuzit, J.-L. et al., Society of Photo-Optical Instrumentation Engineers (SPIE) Conference Series, **7014**, (2008).